ACS APPLIED MATERIALS & INTERFACES

Research Article

www.acsami.org

An Injectable, Calcium Responsive Composite Hydrogel for the Treatment of Acute Spinal Cord Injury

Christopher A. McKay,[†] Rebecca D. Pomrenke,[†] Joshua S. McLane,[‡] Nicholas J. Schaub,[†] Elise K. DeSimone,[†] Lee A. Ligon,[‡] and Ryan J. Gilbert*[,†]

[†]Center for Biotechnology and Interdisciplinary Studies, Department of Biomedical Engineering, Rensselaer Polytechnic Institute, Troy, New York, 12180-3590 United States

[‡]Center for Biotechnology and Interdisciplinary Studies, Department of Biology, Rensselaer Polytechnic Institute, Troy, New York, 12180-3590 United States

Supporting Information

ABSTRACT: Immediately following spinal cord injury, further injury can occur through several secondary injury cascades. As a consequence of cell lysis, an increase in extracellular Ca^{2+} results in additional neuronal loss by inducing apoptosis. Thus, hydrogels that reduce extracellular Ca^{2+} concentration may reduce secondary injury severity. The goal of this study was to develop composite hydrogels consisting of alginate, chitosan, and genipin that interact with extracellular Ca^{2+} to enable in situ gelation while maintaining an elastic modulus similar to native spinal cord (~1000 Pa). It was hypothesized that incorporation of genipin and chitosan would regulate hydrogel electrostatic characteristics and influence hydrogel porosity, degradation, and astrocyte behavior. Hydrogel composition was varied to create hydrogels with statistically similar mechanical properties (~1000 Pa) that demonstrated tunable charge characteristics (6-fold range in free amine concentration) and degradation rate (complete degradation between 7 and 28 days; some blends persist after 28 days). Hydrogels demonstrate high sensitivity to Ca^{2+} concentration, as a 1 mM change during fabrication induced a significant change in elastic modulus. Additionally, hydrogels incubated in a Ca^{2+}-containing solution exhibited an increased linear viscoelastic limit (LVE) and an increased elastic modulus above the LVE limit in a time dependent manner. An extension of the LVE limit implies a change in hydrogel cross-linking structure. Attachment assays demonstrated that addition of chitosan/genipin to alginate hydrogels induced up to a 4-fold increase in the number of attached astrocytes and facilitated astrocyte clustering on the hydrogel surface in a composition dependent manner. Furthermore, Western blots demonstrated tunable glial fibrillary acid protein (GFAP) expression in astrocytes cultured on hydrogel blends, with some hydrogel compositions demonstrating no significant increase in GFAP expression compared to astrocytes cultured on glass. Thus, alginate/chitosan/genipin hydrogel composites show promise as scaffolds that regulate astrocyte behavior and for the prevention of Ca^{2+}-related secondary neuron damage during acute SCI.

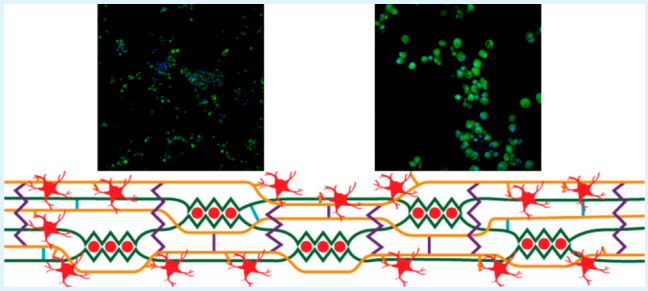

KEYWORDS: *alginate, chitosan, hydrogel, astrocytes, spinal cord injury, glial fibrillary acidic protein*

1. INTRODUCTION

Spinal cord lesions vary in size and severity. However, contusive injuries are most common.[1] Recent reviews reveal interest from the scientific community to develop novel biomaterial hydrogels for spinal cord injury (SCI).[2,3] Hydrogels are ideal scaffolds for the treatment of contusive SCI as many are injectable, conform to the irregular geometry of the contusive lesion and can mimic the mechanical properties of native spinal cord tissue. Following SCI, primary mechanical trauma causes cell swelling and lysis, leading to an increase in extracellular Ca^{2+}.[4] In a rat model of SCI, a 4.1-fold increase in extracellular Ca^{2+} concentration was observed eight hours postinjury and remained stable for at least 72 and up to 168 h postinjury.[5] During subacute SCI, increased extracellular glutamate triggers an influx of Ca^{2+} into neurons[6] leading to an increase in calcium dependent neuronal apoptosis.[7,8] Removal of extracellular Ca^{2+} reverses episodes of glutamate induced excitotoxicity.[9] Furthermore, inhibiting Ca^{2+} influx by blocking Na^{+}-Ca^{2+} exchangers decreases neuronal death.[10] Thus, hydrogels that utilize Ca^{2+} following SCI as a gelation mechanism may aid in hydrogel solidification in situ and potentially reduce Ca^{2+}-induced secondary injury.

Alginate is utilized for tissue engineering applications due to its biocompatibility and low cytotoxicity.[11] Alginate hydrogels have been injected into the adult rat spinal cord, without inciting an inflammatory response.[12] Alginate hydrogels are a good choice for spinal cord applications in that alginate hydrogels form

Received: July 9, 2013
Accepted: January 3, 2014
Published: January 3, 2014

   dx.doi.org/10.1021/am4027423 | ACS Appl. Mater. Interfaces 2014, 6, 1424−1438

through cross-linking with divalent cations. The application of in situ forming hydrogels were recently explored for ophthalmic drug delivery by utilizing Ca^{2+} present within tears.[13] Thus, alginate hydrogels may be able to solidify in situ due to the prevalence of Ca^{2+} in cerebrospinal fluid.

Cellular attachment to a biomaterial surface may occur through inclusion of integrin-mediated focal adhesion complexes or materials that enable electrostatic interactions between the surface and the cellular membrane. However, due to the lack of intrinsic integrin binding sites and its negatively charged character, unmodified alginate exhibits low cellular attachment.[14] Chitosan, an amine-containing, positively charged polysaccharide polymer has been used to alter hydrogel charge within an agarose/methylcellulose hydrogel blend to facilitate cellular adhesion.[15] In addition, genipin, a naturally derived cross-linker, is well suited for use in spinal cord environments as it induces neurite outgrowth,[16] is anti-inflammatory,[17] and has been used to cross-link chitosan containing hydrogel systems without any significant cytotoxicity.[18,19] Genipin reacts with amine groups on chitosan chains and reduces the number of free amine groups available for protonation, decreasing the overall positive charge of the material. Furthermore, an increase in genipin concentration within chitosan containing hydrogels can increase elastic modulus and hydrogel stability.[18] Thus, by varying polymer concentrations, composite hydrogel systems may be created with unique degradation rates, electrostatic character, and cellular adhesion profiles.

Many hydrogel systems demonstrate tunable mechanical properties that can approximate the mechanical properties of soft tissue in the central nervous system (CNS). Control of mechanical behavior is important when developing new hydrogel systems for SCI since neurons exhibit increased neurite branching[20] and neurite extension[21,22] on substrates that mimic the elastic modulus of native CNS tissue (300−1000 Pa).[23,24] By controlling alginate and Ca^{2+} concentrations, alginate hydrogels can be fabricated to mimic the elastic modulus of native CNS tissue.[25] Furthermore, introducing other species to alginate, such as chitosan and genipin, may allow for development of hydrogel systems with elastic moduli similar to native CNS tissue that also exhibit a variety of physical characteristics.

Hydrogels are injected into experimental SCI models for numerous purposes including as a scaffold to support axonal ingrowth across the injury site,[26,27] carrying stem or progenitor cells within the lesion,[28−30] or controlling delivery of therapeutic drugs to mitigate some facet of the injury.[31,32] Hydrogel systems are rarely developed to influence astrocyte behavior although some hydrogel systems demonstrate direct influence on astrocyte behavior.[33] Several studies suggest that the presence of glial support cells, such as astrocytes, is critical for axonal regeneration. For example, increased axonal regeneration is observed following astrocyte migration into biomaterial scaffolds, with axons often migrating parallel to astrocytes.[34−36] Furthermore, hydrogel systems that are not biocompatible with astrocytes may encourage the transition of astrocytes to a reactive state and promote glial scar formation. If a hydrogel system is incompatible with astrocytes and encourages glial scar formation, then functional restoration may be difficult regardless of the efficacy of the hydrogel system in promoting neuronal regeneration.

In this study, it was hypothesized that alginate/chitosan/genipin hydrogels could be developed that respond to the presence of Ca^{2+} within external media at concentrations similar to that in cerebrospinal fluid. By utilizing Ca^{2+} present within the surrounding media to finalize in situ gelation, the amount of Ca^{2+} mediated neuronal cytotoxicity would likely decrease. These hydrogel systems would possess mechanical properties similar to native CNS tissue and differential electrostatic properties to promote astrocyte adhesion. Alginate, chitosan, genipin, and Ca^{2+} concentrations were varied to fabricate hydrogel blends with statistically similar elastic moduli, as determined by small amplitude oscillatory shear (SAOS) rheology. To model in situ hydrogel formation, hydrogel mechanical behavior was characterized using rheological testing following incubation in media containing either normal (1.8 mM) or elevated (6 mM) Ca^{2+} concentrations. To determine the effect of chitosan and genipin on hydrogel electrostatic character, the free amine content within hydrogel blends was determined using a ninhydrin assay. Primary rat astrocytes were cultured on hydrogels to examine the interplay between astrocyte adhesion and hydrogel composition. Additionally, Western blotting was performed on astrocytes cultured on hydrogels to explore how hydrogel composition affects the production of glial fibrillary acidic protein, a key marker of astrocyte reactivity. Furthermore, degradation assays and scanning electron microscopy were used to analyze degradation rate and pore structure and to evaluate their potential for delivery of therapeutic agents.

2. EXPERIMENTAL METHODS

Materials. Genipin was purchased from Wako Pure Chemical (Japan). Alginic acid sodium salt and low molecular weight chitosan (Lot# KBD3830, 92.2% deacetylation) were purchased from Sigma-Aldrich (Saint Louis, MI). Neurobasal media, Dulbecco's Modified Eagle Medium (DMEM), B27 Supplement, penicillin/streptomycin, L-glutamine, Phosphate Buffered Saline (PBS), and Heat Inactivated Horse Serum (HIHS) were purchased from Gibco. Calcein AM and Hoechst 33342 were purchased from Invitrogen. All other chemicals used were purchased from Sigma-Aldrich. Figures were created using SigmaPlot 11 (Systat Software, San Jose CA).

Alginate Hydrogel Fabrication. To make alginate hydrogels, sodium alginate was dissolved in 10 mL of 0.85% NaCl. The sodium alginate solution was mixed for 30 minutes via magnetic stirring with 10 mL of a varying concentration of $CaCl_2$ to produce specific hydrogels. The finalized alginate hydrogel was collected by centrifugation and removal of the supernatant.

Alginate/Chitosan/Genipin Hydrogel Fabrication. Low molecular weight chitosan was dissolved in 6 mL of 0.4% acetic acid. The chitosan solution was neutralized to 7 pH using 0.5 M NaOH. Genipin was added to the neutralized chitosan solution, and the solution was brought to a final volume of 10 mL by addition of 0.85% NaCl. The range of genipin concentrations tested within this study was determined based on previous hydrogel studies that utilized genipin to cross-link chitosan without a significant cytotoxic effect.[18,19] Within this range, genipin concentrations were chosen to fabricate hydrogels with differential cross-linking patterns that exhibited different physical and mechanical properties. The chitosan/genipin solution was incubated at 37 °C for 24 h to induce chitosan/genipin cross-link formation. After 24 h, 5 mL of sodium alginate in 0.85% NaCl was added to the chitosan/genipin solution. The resulting solution was mixed with 5 mL of a varying concentration of $CaCl_2$ for 30 minutes. The $CaCl_2$ concentration was adjusted in order to provide a uniform elastic modulus between all hydrogels. For example, when 0.125% chitosan and 0.1% genipin were added to 0.5% alginate hydrogels, $CaCl_2$ concentration was increased from 22 to 24 mM in order to prevent a significant change in elastic modulus. The finalized hydrogel was collected by centrifugation and removal of the supernatant. To describe the hydrogel compositions used throughout this article, a shorthand naming convention was applied as follows: A hydrogel composed of 0.5% w/v alginate, 0.125% w/v chitosan, 0.1% w/v genipin, and 24 mM $CaCl_2$ is given the name A5/C125/G1/Ca24. Table 1 provides a summary of hydrogel compositions used in this study. Alginate, chitosan, and genipin polymers were sterilized via ethylene oxide

Table 1. Hydrogel Composition[a]

gel type	alginate concn [w/v]	chitosan concn [w/v]	genipin concn [w/v]	$CaCl_2$ concn [mM]
A25/C0/G0/Ca22	0.25%	0%	0%	22
A25/C125/G1/Ca23	0.25%	0.125%	0.1%	23
A25/C25/G05/Ca18	0.25%	0.25%	0.05%	18
A5/C0/G0/Ca22	0.5%	0%	0%	22
A5/C125/G1/Ca24	0.5%	0.125%	0.1%	24
A5/C25/G01/Ca20	0.5%	0.25%	0.01%	20

[a]Calcium concentration was adjusted in order to provide a uniform elastic modulus between hydrogel blends.

sterilization. Acetic acid, NaOH, $CaCl_2$, and NaCl solutions were sterilized via autoclave.

Rheological Characterization. An AR-G2 rheometer (TA Instruments, New Castle, DE) with a parallel plate geometry (20 mm diameter) was used to determine hydrogel viscoelastic behavior. Rheological analysis was performed at 37 °C with a gap size of 1000 μm. For each sample, 500 μL of hydrogel was injected on the rheometer using a 22.5G, 1 mL syringe. Time sweeps were performed at 1% strain with a 1 Hz frequency to determine gelation time at 37 °C. Hydrogel materials are partially gelled prior to testing due to the presence of $CaCl_2$ in the fabrication solution. In the context of this study, gelation time is defined as the point of elastic modulus saturation in response to the change in temperature. Hydrogel gelation was considered complete when no significant difference in elastic modulus was observed compared to the elastic modulus recorded after 60 minutes. For subsequent tests, hydrogels were equilibrated at 37 °C for their respective gelation time. Next, the linear-viscoelastic (LVE) limit for strain was determined by performing a strain sweep from 0.1%−100% at a frequency of 1 Hz. A strain of 1% was below the LVE limit for each hydrogel and was used for all subsequent testing. After determination of the strain LVE limit, frequency sweeps were performed over the range of 0.1−100 Hz using a chosen strain below the LVE limit. The LVE region of the frequency sweep (defined as the region in which the elastic modulus is constant over a range of frequencies) was determined, and a frequency within the LVE region was chosen for subsequent testing. This value was 1 Hz for all hydrogels characterized. Time tests were performed for one hour to determine ultimate elastic modulus (UEM), using the strain and frequency values within their respective LVE regions as previously determined.

To model hydrogel gelation in situ, 500 μL of hydrogels was injected into chamber slides and incubated at 37° C for 2 or 5 days in 200 μL of neurobasal media containing 2% v/v B27 Supplement, 1% v/v penicillin/streptomycin, and 0.5 mM L-glutamine. To observe how the increase in Ca^{2+} concentration following SCI affects hydrogel gelation, two concentrations of $CaCl_2$ were utilized: 1.8 mM (normal) and 6 mM (elevated). Following SCI, Ca^{2+} concentration can increase up to 4.1-fold from normal Ca^{2+} concentrations (1.4 mM), and a Ca^{2+} of 6 mM was used to approximate this value. Furthermore, a Ca^{2+} concentration of 1.8 mM was used for in situ gelation modeling to correspond with the Ca^{2+} concentration in cell culture media.

Three hydrogel blends were chosen for in situ gelation modeling with an elevated Ca^{2+} concentration based on their dominant method of cross-linking: A5/C0/G0/Ca22 (alginate/Ca^{2+}), A5/C125/G1/Ca24 (chitosan/genipin, genipin/genipin), and A5/C25/G01/Ca20 (alginate/chitosan). Media was removed and replaced every 24 h. After the appropriate time point was reached, media was removed, and rheological assessment was performed.

Degradation. There are no endogenous enzymes within the SCI environment to degrade alginate. For alginate-based biomaterials, the dominant form of degradation is caused by the diffusion of Ca^{2+} ions from the hydrogel and subsequent dissolution of alginate polymer chains.[37] To measure hydrogel degradation rate, 500 μL of hydrogel was injected into a 24 well plate. After injection, hydrogel weight was measured, and 200 μL of artificial cerebrospinal fluid (aCSF) was added and replaced every 24 h. The composition of aCSF was as follows: [Na^+] − 150 mM, [K^+] − 3 mM, [Ca^{2+}] − 1.4 mM, [Mg^{2+}] − 0.8 mM, [P] − 1 mM, [Cl^-] − 155 mM.

Hydrogels were allowed to degrade for 0, 1, 3, 5, 7, 10, 14, 21, or 28 days at 37 °C. After the respective time point was reached, the degraded hydrogel was removed, and the wet weight was measured. The wet weight was used to calculate the percent remaining of degraded gels using

$$\%\text{Gel Remaining} = \left(\frac{W_f}{W_0}\right)*100 \qquad \text{(Equation 1)}$$

where W_f is final wet weight and W_0 is initial wet weight. Degraded gels were frozen at −80 °C for 24 h and lyophilized for 24 h, and the dry weight was recorded.

Ninhydrin Assay. To assess hydrogel electrostatic character by measuring the number of free amine groups, a ninhydrin assay was performed as previously described.[38] For the assay, 1 mL of ninhydrin solution was added to 100 μL of hydrogel. This reaction persisted for 20 minutes at 100 °C. After 20 minutes, 200 μL of the reacted solution was removed, and the absorbance value was read at 570 nm using a BioTek Synergy 4 plate reader. A standard glycine curve was used to determine free amine group concentration.

Astrocyte Adhesion Assay. The Institutional Animal Care and Use Committee at Rensselaer Polytechnic Institute approved all procedures in this study involving astrocytes. Astrocytes were isolated from P2 neonatal rat cortex (Sprague-Dawley, P2; Taconic Farms, Inc.) as previously described.[39] Only primary or 1st passage astrocytes were used in this study. To assess astrocyte/hydrogel interaction, 500 μL of hydrogels was injected into chamber well slides (Lab-Tek, Thermo Fisher Scientific, Rochester NY), and astrocytes were seeded at a density of 100,000 cells per well with a total volume of 200 μL of astrocyte media. Astrocyte media consisted of 10% v/v HIHS and 1% v/v penicillin/streptomycin in DMEM. After incubation for 2 days, astrocytes were stained with a mixture of 4 μg/mL of Calcein AM and 10 μg/mL of Hoechst 33342 (diluted in PBS) added in a 1:1 ratio with culture media for 20 minutes and imaged at 10X and 40X using a Zeiss LSM 510 META Laser Scanning Confocal Microscope.

Images of astrocytes labeled with Calcein-AM and Hoechst 33342 were analyzed using a Matlab (MathWorks, Natick, MA) code to determine the number of attached astrocytes, the number of astrocyte cell clusters, and the number of astrocytes per cell cluster. A cell cluster was defined as a region in the Calcein AM channel that overlaps one or more nuclei labeled with Hoechst 33342. The number of cells in a cluster was determined by counting the number of Hoechst 33342 labeled nuclei within a single region labeled for Calcein AM. Individual cell numbers were determined using the Hoechst 33342 signal. To perform the analysis, both the Calcein AM and Hoechst 33342 channels were blurred using a Gaussian filter followed by background subtraction using the sliding paraboloid method. Next, the Calcein AM and Hoechst 33342 channels were segmented using a k-means algorithm using five means. After segmentation by the k-means method, the Hoechst 33342 channel was further segmented using a watershed filter. Finally, a count was performed to determine the number of Hoechst 33342 objects within a single region of the segmented Calcein AM image. Postprocessing was performed on 10X magnification images of both Calcein AM and Hoechst 33342 stained images.

Western Blot Analysis. Protein expression in cultured astrocytes was determined by quantitative Western blot analysis. As described previously, three hydrogel compositions were chosen for Western blot analysis based on their dominant method of cross-linking as well as their astrocyte adhesion response: A5/C0/G0/Ca22, A5/C125/G1/Ca24, and A5/C25/G01/Ca20. Astrocytes were seeded on top of 500 μL of hydrogel injected into 6 chamber slide wells for each hydrogel type at a density of 100,000 cells per well with a total volume of 200 μL of astrocyte media. Furthermore, astrocytes were seeded at the same concentration on poly-D-lysine (PDL) coated glass bottomed, chamber slide wells as a control group. Astrocytes were lysed using RIPA buffer (Sigma-Aldrich, R0278) with the addition of one cOmplete Mini protease inhibitor tablet (Roche Diagnostics, Indianapolis, Indiana) per 10 mL of RIPA buffer. Total protein concentration was determined using the colorimetric QuantiPro BCA Assay Kit (Sigma-Aldrich), and subsequent changes in absorbance were measured using a BioTek

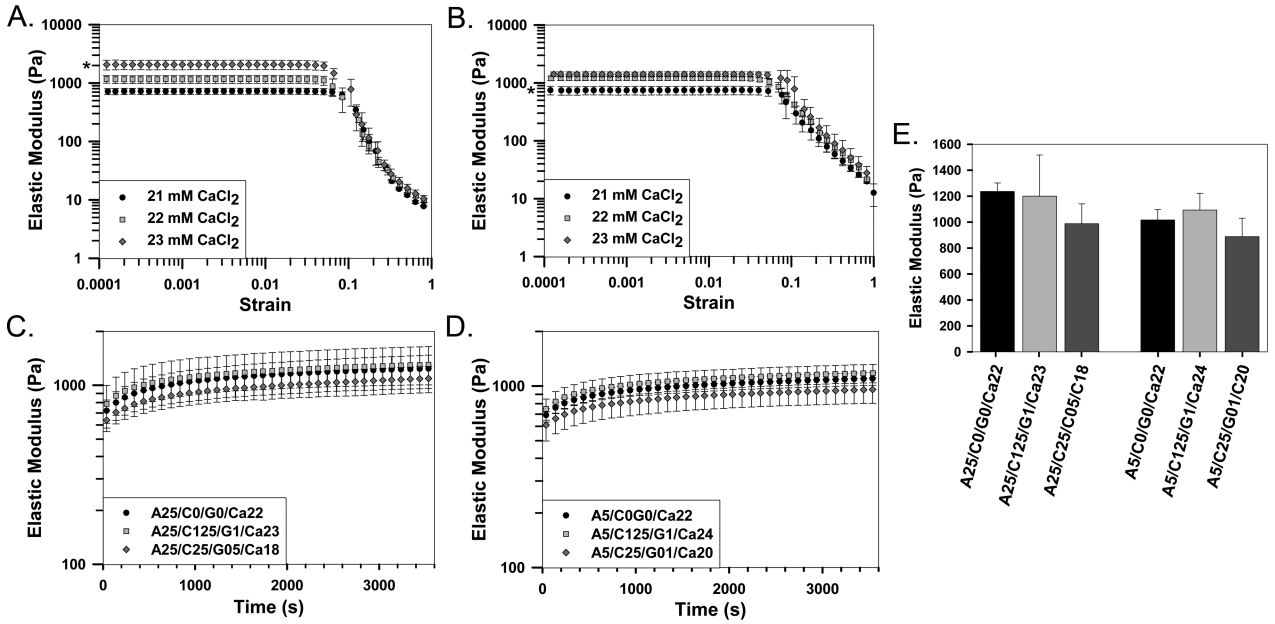

Figure 1. Sensitivity of hydrogel elastic modulus to changes in Ca^{2+} concentration and hydrogel composition. A-B) Strain sweeps demonstrating mM level sensitivity to changes in Ca^{2+} concentration for (A) 0.25% or (B) 0.5% alginate hydrogels. C-D) Gelation time tests demonstrating gelation kinetics for alginate or composite hydrogels with a base of (C) 0.25% or (D) 0.5% alginate. E) Comparison of elastic modulus of all hydrogels 30 minutes after beginning of the gelation time tests. $n = 3$, mean ± standard deviation. (* denotes statistically significance differences between all groups.)

Synergy 4 plate reader. Protein solutions were diluted in a 1:1 ratio with sample buffer (0.125% w/v bromophenol blue, 25% v/v glycerol, 2.5% w/v SDS, 20 mM dithiotheritol, and 25 mM Tris at a pH of 6.8) and frozen at −20 °C until utilized for the assay. Protein was loaded into a 10% polyacrylamide gel, separated via SDS-PAGE, and transferred onto a polyvinylidene difluoride (PVDF) membrane for immunoblotting. Following protein transfer, membranes were blocked with 0.5% w/v milk in Tris-buffered saline containing 0.05% v/v Tween 20 (TBST) for 1 h. Membranes were incubated at 4 °C with anti-GFAP antibody (1:15,000, Sigma-Aldrich, SAB2500462), washed three times with TBST for 1 hour, and subsequently incubated with an appropriate horseradish peroxidase (HRP)-conjugated secondary antibody (1:100,000, Jackson ImmunoResearch, West Grove, PA). HRP signal was detected using an Immun-Star WesternC Chemiluminescence Kit (Bio-Rad, Hercules, CA). Following imaging of the GFAP signal, PVDF membranes were subsequently stripped of antibodies and reprobed with an anti-α-tubulin antibody (Sigma-Aldrich, Saint Louis, MO, T6199) and a corresponding HRP-conjugated secondary antibody (1:100,000, Jackson ImmunoResearch, West Grove, PA) to ensure equal levels of protein loading. Quantitative analysis was performed on Western blots using protein isolated from three independent cultures ($n = 3$) using the Analyze>Gels function of ImageJ (U.S. National Institute of Health, Bethesda, MD). For quantification, intensity levels of each GFAP band were normalized to the intensity of their respective α-tubulin band. Furthermore, all GFAP/α-tubulin intensity ratios were divided by the average GFAP/α-tubulin intensity ratio of the glass control group in order to a) normalize the average value of the control group to a value of 1 and b) provide experimental GFAP/α-tubulin tubulin intensity ratios as a fold-increase relative to the glass control. An experimenter blinded to the different groups performed all Western blot experiments and quantification.

Scanning Electron Microscopy. Scanning electron microscopy was performed on hydrogels to observe gel morphology and porosity. Hydrogels were frozen for 24 h at −80 °C and lyophilized for 24 h. A cross-section of the hydrogel sample was mounted to aluminum stubs with carbon tape. Samples were sputter coated at 25% for 60 s using a Denton Desk V sputter coater with a platinum target. Hydrogel samples were imaged using a Zeiss SUPRA 55 FESEM with an accelerating voltage of 3 kV.

Statistical Analysis. All error bars denote the mean plus or minus the standard deviation. All experiments were performed on three independently fabricated samples on separate days. For astrocyte image analysis, three images were captured from each sample and image analysis was performed as previously described. Data from each sample was pooled prior to statistical analysis, providing an $n = 3$ for each group. Statistical significance between groups was determined by one-way ANOVA and Tukey-Kramer HSD tests using JMP software (SAS, Cary NC). Differences were considered significant for $p < 0.05$.

3. RESULTS

Sensitivity of Alginate Hydrogels to Changes in Ca^{2+} Concentration. To evaluate the sensitivity of elastic modulus to variations in Ca^{2+} concentration, strain sweeps were performed on alginate hydrogels fabricated using differing amounts of $CaCl_2$ (Figure 1). Rheological analysis of alginate hydrogels revealed a decreasing elastic modulus in response to a 1 mM incremental decrease in the concentration of $CaCl_2$ (Figures 1A and 1B). For 0.25% alginate hydrogels, a significant decrease in elastic modulus was observed when $CaCl_2$ concentration was decreased from 23 to 22 mM (23 mM: 2072 ± 376 Pa, 22 mM: 1165 ± 179 Pa; Figure 1A). Similarly, for 0.5% alginate hydrogels, the elastic modulus was significantly decreased when $CaCl_2$ concentration was decreased from 22 to 21 mM (22 mM: 1211.3 ± 102.7 Pa, 21 mM: 745 ± 126.4 Pa; Figure 1B). However, no significant difference in elastic modulus was observed when $CaCl_2$ concentration was changed from 22 to 21 mM for 0.25% hydrogels or from 22 to 23 mM for 0.5% hydrogels.

Gelation time tests were performed to examine the influence of physiological temperature on hydrogel formation and to determine how hydrogel composition affects elastic modulus. Results demonstrate that complete gelation occurred within 30 minutes for all hydrogels (Figure 1C and 1D). The concentration of $CaCl_2$ within each hydrogel was adjusted prior to testing to ensure that no significant difference in elastic modulus was observed between hydrogel blends 30 minutes after the start of gelation time tests (Figure 1E).

Rheological Behavior of Hydrogels Following an in Situ Model of Hydrogel Gelation. To model in situ hydrogel

dx.doi.org/10.1021/am4027423 | ACS Appl. Mater. Interfaces 2014, 6, 1424−1438

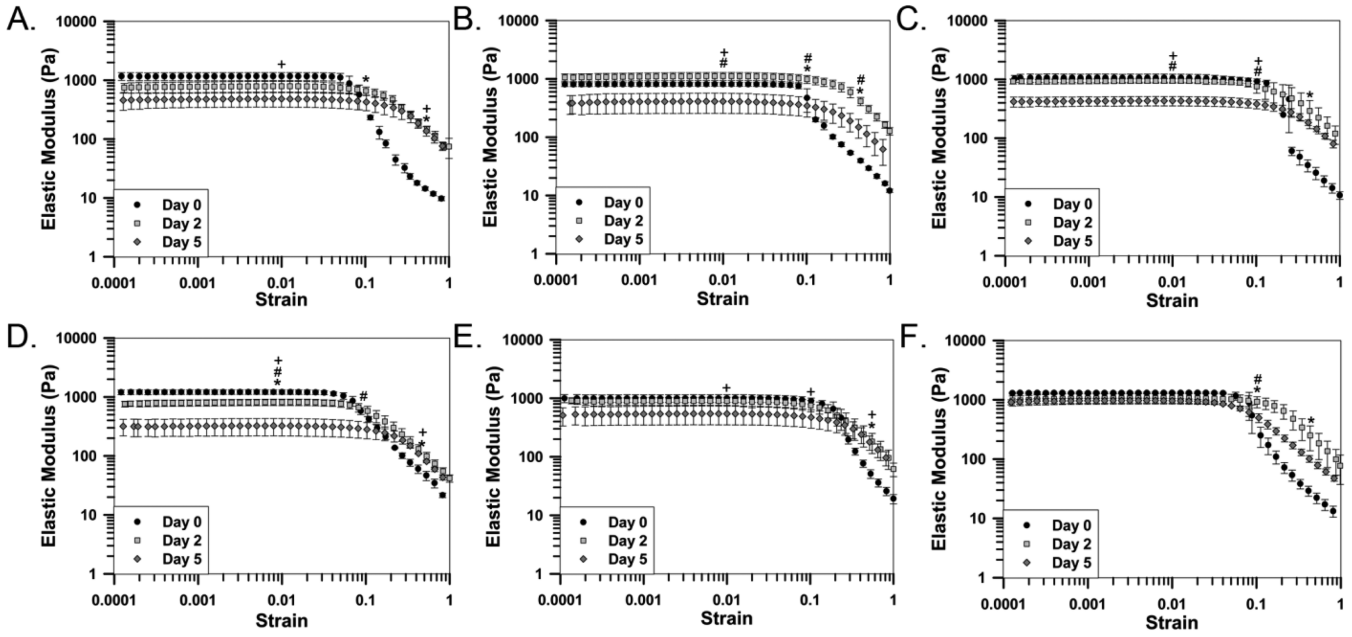

Figure 2. Changes in rheological behavior of hydrogels following in situ gelation modeling with a normal (1.8 mM) Ca^{2+} concentration. Strain sweeps demonstrating the effect of incubation in Ca^{2+} containing media on (A) A25/C0/G0/Ca22, (B) A25/C125/G1/Ca23, (C) A25/C25/G05/Ca18, (D) A5/C0/G0/Ca22, (E) A5/C125/G1/Ca24, and (F) A5/C25/G01/Ca20 hydrogels. $n = 3$, mean ± standard deviation. (* denotes significance between day 0 and day 2. + denotes significance between day 0 and day 5. # denotes significance between day 2 and day 5.)

response to cerebrospinal fluid (CSF) within a spinal cord lesion, hydrogels were incubated for two or five days in neurobasal media containing similar Ca^{2+} concentrations to that observed in CSF before and after injury (1.8 and 6 mM, respectively). Following incubation, rheological testing was performed, and results were compared to nonincubated controls (Figure 2, Supplementary Figure 3). For hydrogels incubated with 1.8 mM Ca^{2+}, no significant change in elastic modulus was observed at 1% strain (below the LVE for all hydrogels) two days following incubation for all hydrogels, with the exception of the 0.5% alginate hydrogel (Figure 2). For 0.5% alginate hydrogels, addition of 0.125% chitosan and 0.1% genipin increases elastic modulus at 1% strain following five days of incubation compared to alginate hydrogels (Figures 2D and 2E). Furthermore, addition of 0.25% chitosan and 0.01% genipin to 0.5% alginate hydrogels prevents a decrease in elastic modulus at 1% strain that is observed in 0.5% alginate hydrogels (Figures 2D and 2F). Conversely, the same behavior was not observed in hydrogels with a base of 0.25% alginate. The elastic modulus of all hydrogels containing 0.25% alginate significantly decreased after five days of incubation when compared to nonincubated samples (Figures 2A, 2B, and 2C).

Following incubation, hydrogels exhibited a shift in the LVE limit towards higher strain values compared to nonincubated samples (Figure 2). Hydrogels that exhibit no significant change in elastic modulus at 1% strain after two days of incubation exhibit a significantly higher elastic modulus at 50% strain and a shift in the LVE limit towards a higher strain magnitude (Figure 2). Following five days of incubation, a statistical difference in elastic modulus was not always observed at 50% strain in hydrogels exhibiting a shift in the LVE limit, due to a decrease in elastic modulus above the LVE limit. However, a shift in the LVE limit was observed in all hydrogels incubated for two or five days compared to nonincubated hydrogels. The shift indicates that incubation induced changes in hydrogel structure is maintained over time and is not lost with a decrease in elastic modulus (Figure 2). Analysis of viscous modulus (Supplementary Figure 1) and phase angle (Supplementary Figure 2) data support the results presented in Figure 2. A delay in the increase in both viscous modulus and phase angle in response to an increase in applied strain is observed following in situ gelation modeling, indicating more stable and solidlike hydrogel behavior compared to nonincubated hydrogels. Additionally, similar results are observed following in situ gelation modeling of hydrogels with media containing elevated Ca^{2+} concentrations (6 mM; Supplementary Figure 3).

Frequency sweeps were performed on all hydrogels to determine a frequency value for which each hydrogel blend behaves in a linear viscoelastic manner. A frequency of 1 Hz was within the LVE region for all hydrogel blends, pre- and postincubation, and was chosen as a suitable frequency for further testing (data not shown). Time tests were performed to determine the ultimate elastic modulus (UEM) of hydrogel blends after incubation in media containing either low (normal) or high (elevated) concentrations of Ca^{2+} (Figure 3). The change in UEM after incubation is dependent on incubation time, hydrogel composition, and Ca^{2+} concentration within the incubation solution. The UEM of all hydrogel blends significantly decreases following 5 days of incubation in media containing a low concentration of Ca^{2+}. Conversely, incubation in media containing a high concentration of Ca^{2+} prevents a significant decrease in UEM at both day 2 and day 5 time points. The UEM of 0.5% alginate hydrogels drops significantly following incubation in media with low Ca^{2+} concentration, and a significant difference in UEM is observed between high and low Ca^{2+} concentrations at day 2 and day 5 (Figure 3A). Composite hydrogels display a similar trend to that observed in alginate hydrogels, in a manner dependent on chitosan and genipin concentration (Figures 3B and 3C). However, the rate of decrease in hydrogel UEM after incubation in low Ca^{2+} media is significantly slowed in composite hydrogels, compared to alginate hydrogels. While a significant difference in UEM is observed after two days of incubation in low Ca^{2+} media (compared to day 0 low Ca^{2+} and all

dx.doi.org/10.1021/am4027423 | ACS Appl. Mater. Interfaces 2014, 6, 1424−1438

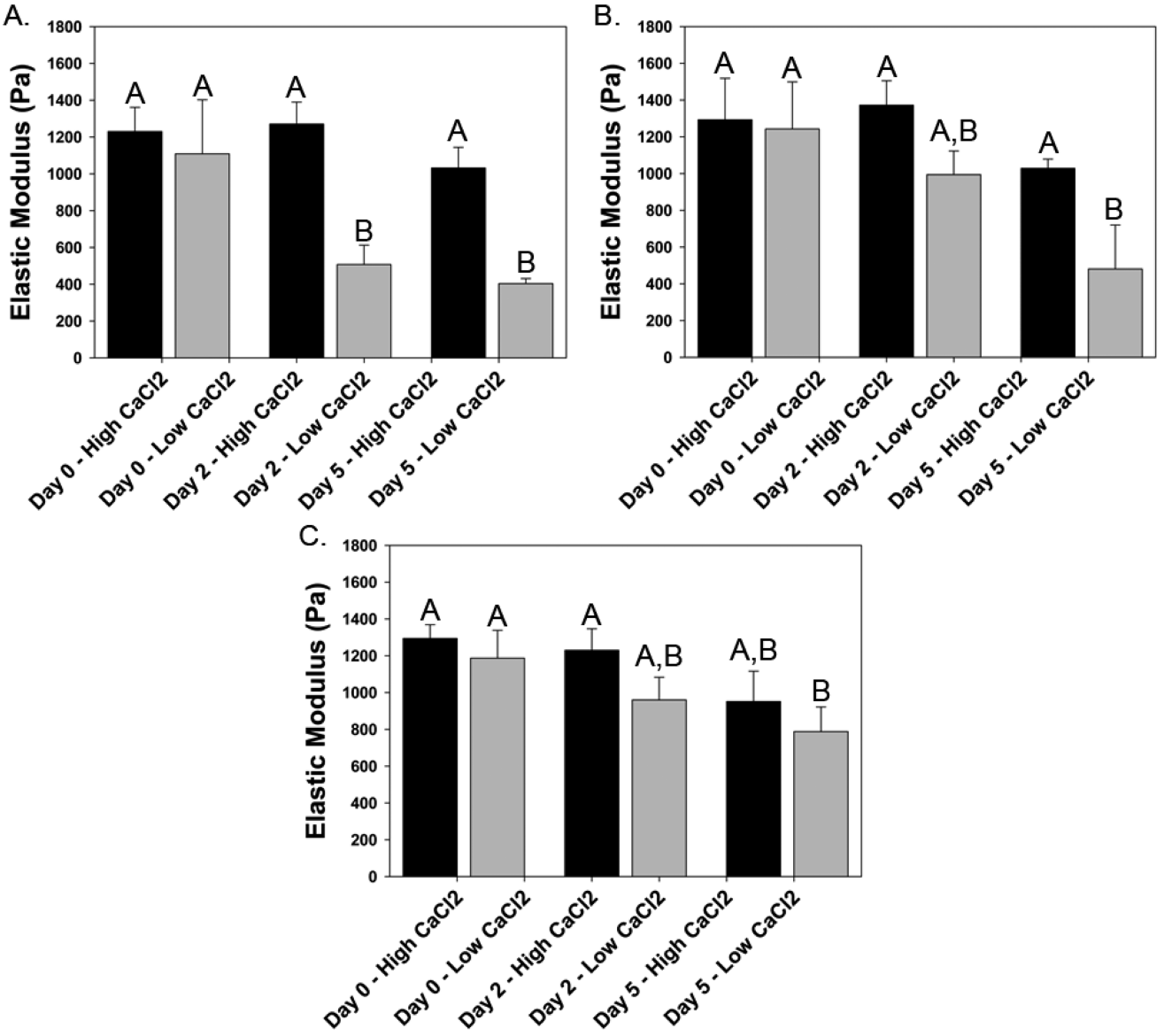

Figure 3. Comparison of the change in ultimate elastic modulus following in situ gelation modeling for low and high calcium concentrations. Time tests demonstrating the effect of incubation in media containing low (normal) and high (elevated) Ca^{2+} concentrations for (A) A5/C0/G0/Ca22, (B) A5/C125/G1/Ca24, and (C) A5/C25/G01/Ca20 hydrogels. $n = 3$, mean ± standard deviation. (Bars with the same letters represent groups in which no statistical differences were observed, while bars with different letters are statistically different from one another.)

high Ca^{2+} hydrogels), no significant difference in UEM was observed after two days in incubation for all composite hydrogels tested. Furthermore, for hydrogels containing 0.125% chitosan and 0.1% genipin, a significant difference in UEM was observed after five days of incubation in low Ca^{2+} media when compared to all high Ca^{2+} time points. However, when chitosan and genipin concentrations were changed (0.25% and 0.01%, respectively), no statistical difference was observed at day 5 for hydrogel incubated in low and high Ca^{2+} media. It is noteworthy that the UEM of day five hydrogels remains within the range (300−1000 Pa)[23,24] exhibited by CNS tissue.

Effect of Hydrogel Composition on Hydrogel Degradation Rate. Since our hydrogel is designed to interact with CSF Ca^{2+} to reduce the impact of secondary excitotoxic neuronal damage and facilitate astrocyte adhesion as the injury site stabilizes, it is desirable for the hydrogel to persist through the subacute phase of SCI. Therefore, an in vitro degradation study was performed to determine the effect of chitosan concentration and hydrogel composition on the degradation rate of hydrogels within aCSF ($[Na^+]$ − 150 mM, $[K^+]$ − 3 mM, $[Ca^{2+}]$ − 1.4 mM, $[Mg^{2+}]$ − 0.8 mM, [P] − 1 mM, $[Cal^-]$ − 155 mM) (Table 2). Alginate hydrogels degraded more quickly than composite hydrogels. For 0.25% and 0.5% alginate gels, 35% and 25% of the initial wet weight was lost within the first day, respectively. Comparatively, composite hydrogels exhibited significantly less degradation (greater than 95% and 90% of wet weight remained at days 1 and 5, respectively) than alginate hydrogels. Alginate hydrogels were completely degraded by day 14, while at least 80% of the hydrogel wet weight remained after 14 days for composite hydrogels. All hydrogels with at least a 0.05% genipin content degraded quickly after day 14, becoming fully degraded before day 21. The only hydrogel to remain intact throughout the entire 28 day study contained the highest alginate and chitosan concentrations and the lowest genipin concentration (A5/C25/G01/Ca20). Detailed degradation profiles are provided in Supplementary Figure 4.

dx.doi.org/10.1021/am4027423 | ACS Appl. Mater. Interfaces 2014, 6, 1424−1438

Table 2. Hydrogel Wet Weight Degradation[a]

	% gel remaining					
time point (days)	A25/C0/G0/Ca22	A25/C125/G1/Ca23	A25/C25/G05/Ca18	A5/C0/G0/Ca22	A5/C125/G1/Ca24	A5/C25/G01/Ca20
1	65 ± 11	99 ± 3[b]	99 ± 3[b]	76 ± 3	104 ± 3[b]	95 ± 3[b,c]
5	54 ± 3	98 ± 1[b]	90 ± 4[b]	79 ± 6	100 ± 2[b]	97 ± 5[b]
14	0	82 ± 5[b]	92 ± 2[b,c]	0	85 ± 3[b]	95 ± 4[b]
28	0	0	0	0	0	60 ± 14[b,c]

[a]Values are provided as percentage of hydrogel remaining. n = 3, mean ± standard deviation. [b]Denotes significance between hydrogels with and without chitosan/genipin. [c]Denotes significance between alginate/chitosan/genipin hydrogels with fixed alginate and differing chitosan concentrations).

Effect of Hydrogel Composition on Free Amine Content within Composite Hydrogels. Amine containing polymers are used in several hydrogel applications to improve cellular adhesion.[15,26,40,41] To measure the amount of free amine groups within composite hydrogels, ninhydrin assays were performed. By determining the amount of free amine groups, the relative positive charge character of each hydrogel sample can be determined.

Ninhydrin assays demonstrate a significant difference in free amine group concentration within composite hydrogels in a composition dependent manner (Figure 4). For hydrogel blends

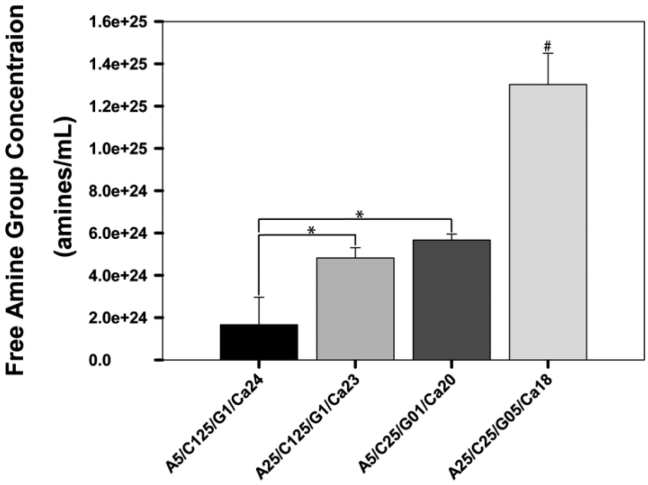

Figure 4. Ninhydrin Assay. The number of free amine groups within composite hydrogels is composition dependent. An increase in chitosan concentration and decrease in genipin concentration leads to an increase in the number of free amine groups. n = 3, mean ± standard deviations (* denotes significance between connected groups. # denotes significance between all groups.)

with a fixed alginate concentration, an increase in chitosan concentration and decrease in genipin concentration provide a significant increase in free amine group concentration (2.7- and 3.4-fold increase for 0.25% and 0.5% alginate hydrogels, respectively). Similarly, for hydrogel blends with fixed chitosan and genipin concentration, a decrease in alginate concentration resulted in a significant increase in free amine group concentration (2.9-fold increase for 0.125% chitosan hydrogels). Interestingly, for hydrogels where chitosan concentration is fixed, alginate concentration is decreased, and genipin concentration is increased, a significant increase in the concentration of free amine groups is observed (2.3-fold increase for 0.25% chitosan hydrogels).

Visualization of External Hydrogel Appearance and Internal Hydrogel Structure. The external appearance (Figure 5; left) and internal structure (Figure 5; right) of all hydrogels were examined. Alginate hydrogels exhibit a transparent appearance (Figures 5A and 5B), while the addition of chitosan/genipin to hydrogels induces a blue hue in a manner dependent on genipin concentration (Figures 5C-5F). Hydrogels fabricated with 0.125% chitosan and 0.1% genipin exhibit a dark blue hue (Figures 5C and 5D). An increase in chitosan and decrease in genipin to 0.25% and 0.05%, respectively, appears to induce a slight lightening in hydrogel color (Figure 5E). However, a further decrease in genipin concentration (0.01% genipin; Figure 5F) produces a significantly lighter hydrogel, which is light blue/green in appearance.

Scanning electron microscopy (SEM) images of the hydrogels revealed a highly porous network (Figure 5; right). The addition of chitosan/genipin appears to impact the number of pores as well as their size in a concentration dependent manner. The addition of 0.125% chitosan and 0.1% genipin appears to produce a more open hydrogel morphology, with less pores of greater size (Figures 5C and 5D). However, a further increase in chitosan and decrease in genipin produces a hydrogel structure containing a larger number of pores with smaller diameters (Figures 5E and 5F), more closely resembling the structure of alginate hydrogels. Pore size for all hydrogels is large enough to allow for diffusion of media into the interior of the hydrogel, as evidenced by the presence of phenol red within the interior of the hydrogel during incubation experiments (data not shown).

Attachment Assays Demonstrate Composition Dependent Astrocyte Attachment and Clustering on the Surface of Hydrogels. The addition of chitosan/genipin to alginate hydrogels significantly affects the number of astrocytes attached to the hydrogel surface as well as influences the incidence of astrocyte clustering (Figure 6). Figures 6A-6C show the proposed cross-linking mechanisms and observed cellular interaction within alginate hydrogels (Figure 6A), composite hydrogels with low chitosan and high genipin concentration (Figure 6B), and composite hydrogels with high chitosan concentration and low genipin concentration (Figure 6C). Figures 6D-6F show fluorescent images of cells cultured on hydrogels at 10X magnification, and Figures 6G-6I show fluorescent images of cells cultured on hydrogels at 40X magnification for alginate hydrogels (A25/C0/G0/Ca22; Figures 6D and 6G), composite hydrogels with low chitosan and high genipin concentration (A25/C125/G1/Ca23; Figures 6E and 6H), and composite hydrogels with high chitosan and low genipin concentration (A25/C25/G05/Ca18; Figures 6F and 6I). Image analysis was performed on 10X magnification images for all hydrogel blends in order to determine the number of astrocytes attached to the hydrogel surface (Figure 6J) and determine the extent of cell cluster formation (Figure 6K) and the number of cells within each cell cluster (Figure 6L). This is done to provide

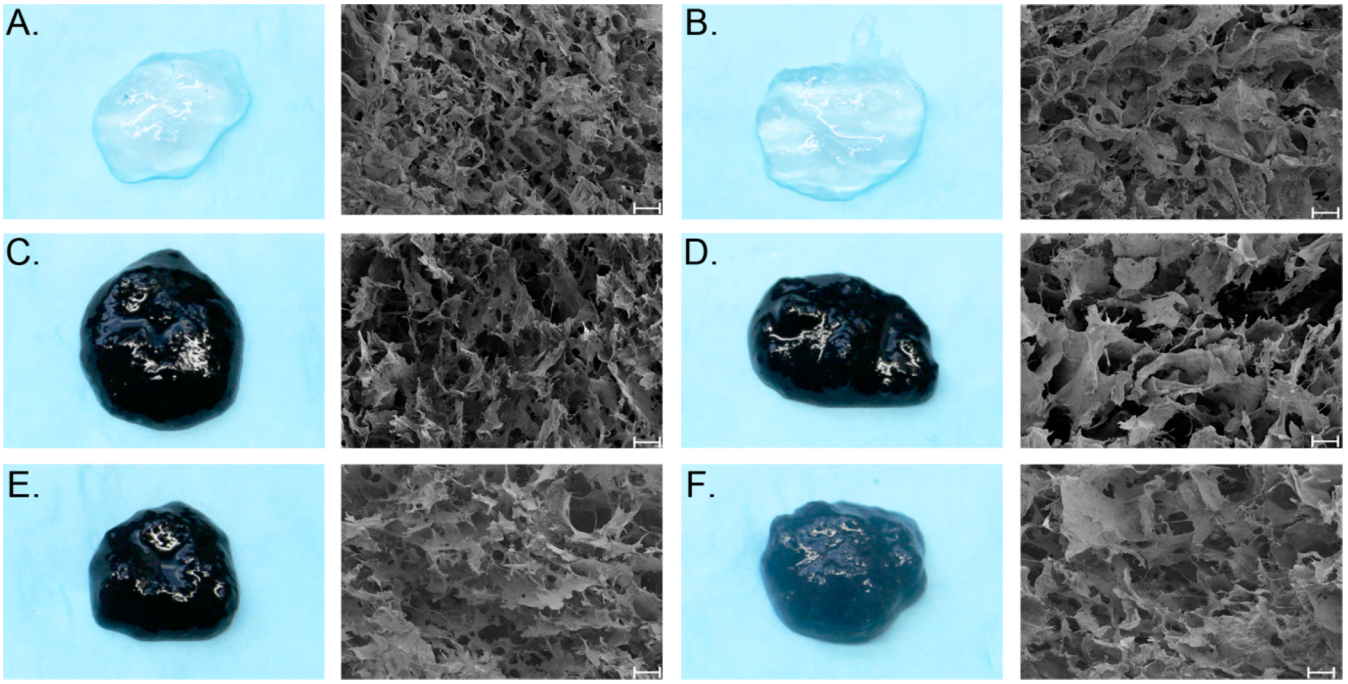

Figure 5. Images (left) and scanning electron micrographs (SEM; right) of alginate and composite hydrogels. A) A25/C0/G0/Ca22, B) A5/C0/G0/Ca22, C)A25/C125/G1/Ca23, D) A5/C125/G1/Ca24, E) A25/C25/G05/Ca18, and F) A5/C25/G01/Ca20. For SEM micrographs: magnification −300X, scale bar −100 μm.

an estimate of how densely cells pack together or spread out along the hydrogel surface.

The addition of chitosan and genipin to alginate hydrogels significantly increased the number of astrocytes attached to the surface of hydrogel blends, in a concentration dependent manner (Figure 6J). Astrocytes cultured on alginate hydrogels demonstrate the lowest amount of cellular adhesion (298 ± 50.5 and 260 ± 57.8 cells/sample for 0.25% and 0.5% alginate hydrogels, respectively), with the exception of A5/C25/G01/Ca20 hydrogels (422 ± 77.8 cells/sample). The addition of 0.125% chitosan and 0.1% genipin to 0.25% alginate hydrogels significantly increases the number of astrocytes attached to the hydrogel surface (1253 ± 91.8 cells/sample). Increasing the alginate concentration in these hydrogels decreases the number of attached astrocytes (795 ± 95.5 cells/sample). However, a further increase in chitosan concentration along with a decrease in genipin concentration significantly decreases the number of attached astrocytes when alginate concentration is kept constant (715 ± 172 and 422 ± 77.8 cells/sample for 0.25% and 0.5% alginate hydrogels, respectively).

Images were also analyzed to determine the clustering patterns of astrocytes on the surface of each type of hydrogel blend (Figure 6K). Astrocytes cultured on alginate hydrogels form a relatively small number of clusters on the hydrogel surface (74 ± 4.6 and 70 ± 16.1 clusters/sample for 0.25% and 0.5% alginate hydrogels, respectively). Astrocytes cultured on hydrogels containing 0.25% chitosan formed a statistically similar number of cell clusters compared to alginate hydrogels (66 ± 10.5 and 55 ± 9.3 clusters/sample for 0.25% and 0.5% alginate hydrogels, respectively). However, hydrogels fabricated with 0.125% chitosan and 0.1% genipin exhibited a significantly higher number of cell clusters when compared to all other hydrogels (383 ± 52.7 and 198 ± 41.1 clusters/sample for 0.25% an 0.5% alginate hydrogels, respectively).

Astrocytes cultured on alginate hydrogels exhibit a small number of cells/cluster (Figure 6L; 12 ± 2.3 and 12.5 ± 5.3 cells/cluster/sample for 0.25% and 0.5% alginate hydrogels, respectively) and appear to prefer to cluster together on the hydrogel surface (Figures 6D and 6G). Hydrogels fabricated with 0.25% chitosan exhibit an increase in astrocyte attachment but no change in the number of clusters compared to alginate hydrogels, and thus astrocytes exhibit a high number of cells/cluster on these hydrogel surfaces (33.5 ± 8.1 and 25.2 ± 4.7 cells/cluster/sample for hydrogels containing 0.25% and 0.5% alginate, respectively). Similar to alginate hydrogels, astrocytes on hydrogels containing 0.25% chitosan tend to form dense clusters rather than spread out across the entirety of the hydrogel surface (Figures 6F and 6I). In contrast, astrocytes cultured on hydrogels containing 0.125% chitosan form a large number of clusters containing a relatively small number of cells (10.1 ± 1 and 12.2 ± 1.1 cells/cluster/sample for 0.25% and 0.5% alginate hydrogels, respectively) and spread out along the entirety of the hydrogel surface (Figures 6E and 6H). The schematics in Figures 6A-6C detail the proposed cross-linking mechanisms within each type of hydrogel and how this cross-linking behavior influences astrocyte attachment to the hydrogel surface.

Protein Analysis Demonstrates Composition Dependent GFAP Expression in Astrocytes Cultured on the Surface of Hydrogels. Hydrogel composition has a significant effect on the GFAP expression of astrocytes cultured on hydrogel surfaces, in a composition dependent manner (Figure 7). Figure 7A shows representative Western blots for the intermediate filament GFAP, a protein that has been strongly linked to the formation of reactive astrocytes in SCI, and the loading control protein α-tubulin. Bands for the target GFAP protein (indicated by an arrow) as well as extraneous bands due to nonspecific antibody binding can be observed in the blots for certain groups (Figure 7A). Figure 7B shows the results of Western blot quantification displayed as the intensity ratio of

dx.doi.org/10.1021/am4027423 | ACS Appl. Mater. Interfaces 2014, 6, 1424−1438

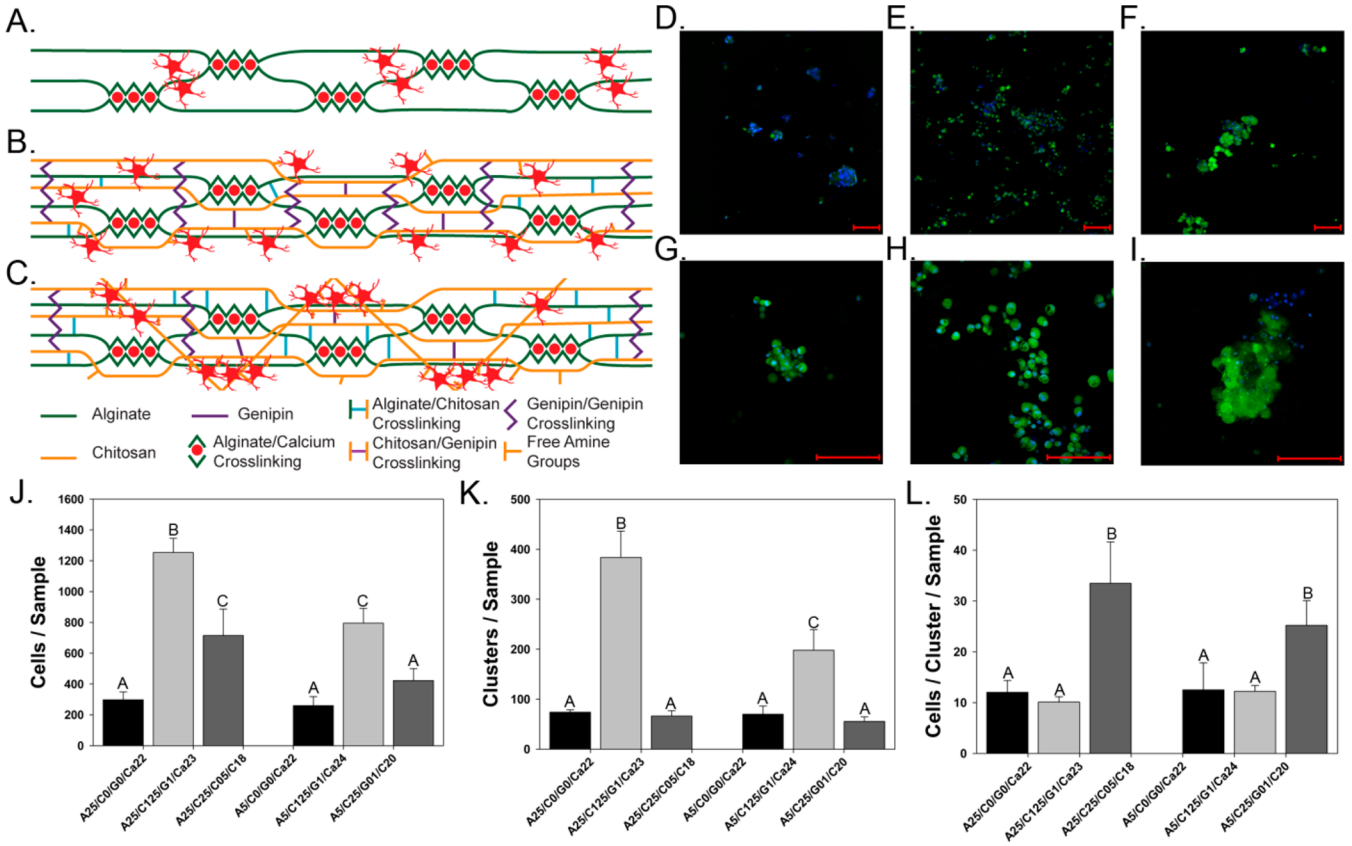

Figure 6. Astrocyte interaction within different hydrogel blends. A-C) Schematics detailing the proposed internal cross-linking nature of hydrogels and cellular interaction for A) alginate hydrogels, B) composite hydrogels with low chitosan and high genipin concentrations, and C) composite hydrogels with high chitosan and low genipin concentration. D-I) Representative fluorescent images of astrocytes attached to different hydrogel blends: D,G) A25/C0/G0/Ca22, E,H) A25/C125/G1/Ca23, and F,I) A25/C25/G05/Ca18 (D-F: 10X Magnification, scale bar −300 μm G-I: 40X Magnification, scale bar −100 μm. Green − Calcein AM, Blue − Hoechst 33342. J-L) Analysis performed on 10X fluorescence images detailing J) the number of cells per sample, K) the number of clusters per sample, and L) the number of cells per cluster per sample for each hydrogel blend. n = 3, mean ± standard deviation (Bars with the same letters represent groups in which no statistical differences were observed, while bars with different letters are statistically different from one another.)

GFAP bands to α-tubulin bands, normalized to the expression of astrocyte seeded on poly-D-lysine (PDL) coated glass substrates.

Astrocyte expression of GFAP is significantly affected by the surface on which they are grown (Figure 7). Astrocytes grown on PDL-coated glass exhibit the least GFAP expression, on average, when compared to astrocytes cultured on all hydrogel surfaces (Figure 7B). However, astrocytes cultured on alginate hydrogels exhibit no significant increase in GFAP expression, compared to astrocytes cultured on PDL-coated glass (1.13 ± 0.79-fold increase). The concentration of chitosan/genipin added to alginate hydrogels has a significant effect on the GFAP expression in astrocytes that are cultured on top of composite hydrogels. The addition of 0.25% chitosan and 0.01% genipin to 0.5% alginate hydrogels results in a slight (but not statistically significant) increase in the average GFAP expression of cultured astrocytes, compared to astrocytes cultured on 0.5% alginate hydrogels and PDL-coated glass (1.41 ± 0.58-fold increase, relative to PDL-coated glass). A decrease in chitosan concentration (0.25% to 0.125%) combined with an increase in genipin concentration (0.01% to 0.1%) induces a significant increase in GFAP expression, compared to both PDL-coated glass and 0.5% alginate hydrogels (2.58 ± 0.23-fold increase, relative to PDL-coated glass). However, there is no significant difference in GFAP expression in astrocytes cultured on chitosan/genipin containing hydrogels (1.41 ± 0.58 and 2.58 ± 0.23-fold increase, relative to PDL-coated glass for composite hydrogels containing 0.25%/0.01% and 0.125%/0.1% chitosan/genipin, respectively).

4. DISCUSSION

Hydrogel Gelation Mechanisms and Charge Characteristics. Alginate/chitosan/genipin biomaterial systems have been previously utilized for the production of microcapsules for oral drug delivery[42] as well as stiff hydrogel discs for the delivery of drugs within the gastric system using N,O-carboxymethyl chitosan.[43] However, these materials were designed for use as drug delivery scaffolds, without regard to their mechanical properties and cellular interaction. In this study, we report a novel fabrication technique for the manufacture of a soft, injectable hydrogel capable of responding to millimolar changes in Ca^{2+} concentration in an in situ gelation model. By controlling the degree of different types of cross-linking, elastic moduli can be maintained and degradation rate, charge character, pore structure, and astrocyte interaction can be tuned by altering hydrogel composition. There are four types of cross-linking exhibited within composite hydrogels in this study: alginate/Ca^{2+}, alginate/chitosan, chitosan/genipin, and genipin/genipin. Alginate cross-links with divalent cations such as Ca^{2+} by sequestering Ca^{2+} between guluronic acid residues to bind together polymer chains.[44,45] The properties of the resulting gel

dx.doi.org/10.1021/am4027423 | ACS Appl. Mater. Interfaces 2014, 6, 1424−1438

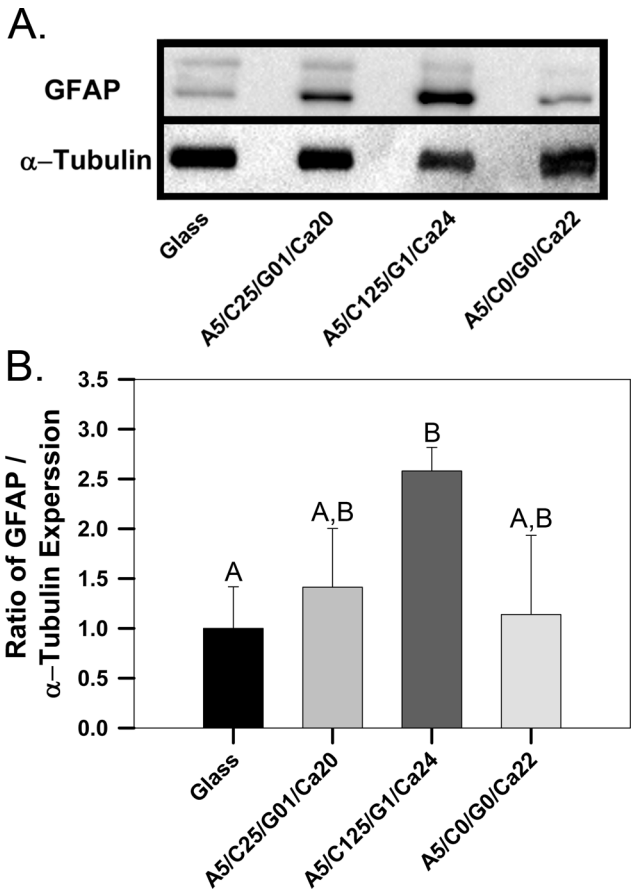

Figure 7. GFAP expression in astrocytes cultured on different hydrogels. A) Representative Western blots showing the GFAP and α-tubulin expression in astrocytes cultured on poly-D-lysine coated glass or hydrogels with different polymer compositions. B) Quantitative analysis performed on Western blots demonstrating the relative GFAP expression in astrocytes cultured on different surfaces. $n = 3$, mean $\pm$ standard deviation. (Bars with the same letters represent groups in which no statistical differences were observed, while bars with different letters are statistically different from one another.)

are dependent on alginate concentration, co-polymer ratio, molecular weight, and Ca^{2+} concentration. Naturally, this method of cross-linking is limited by the amount of available cross-linking sites, implying a theoretical saturation point where the addition of further Ca^{2+} will no longer enable cross-linking to occur within the hydrogel.[25]

Additional cross-linking occurs between chitosan and alginate due to the precipitation of alginate/chitosan polyelectrolyte complexes.[46] Alginate/chitosan polyelectrolyte complex formation is proposed to occur by charge neutralization of the carboxyl and amine groups on alginate and chitosan backbones, respectively.[47] It is possible that polyelectrolyte complex formation may occur between amine groups on the chitosan chain and carboxyl groups on guluronic acid residues, interfering with the potential for alginate to cross-link with divalent cations such as Ca^{2+}.

The addition of genipin adds another dimension of cross-linking within hydrogels. Genipin induces cross-linking within hydrogels fabricated from many different types of polymers including collagen, chitosan, and fibrin.[48,49] Genipin forms cross-links through a reaction with primary amine groups to produce a secondary form of genipin that exhibits a strong blue color.[50] The rigid structure enforced on chitosan chains by covalent cross-linking limits access to ionic binding sites and may limit the potential for alginate/chitosan polyelectrolyte formation.[18] However, this effect is dependent on genipin concentration, as the amount of free amine groups is decreased as the amount of genipin is increased. Furthermore, genipin has the ability to cross-link with itself and form polymerized genipin chains of varying length.[51] This allows for a variety of chemical cross-link patterns between chitosan chains that increase resistance to degradation by reducing access to enzymatic degradation sites.

For each hydrogel blend, the Ca^{2+} concentration within the hydrogel was adjusted during fabrication in order to provide the desired elastic modulus. It is possible that addition of chitosan and genipin to alginate hydrogels limits efficiency of alginate/Ca^{2+} binding by limiting the number of consecutive alginate/Ca^{2+} binding sites through chain entanglements and alginate/chitosan polyelectrolyte complex formation. The relatively high genipin concentration in hydrogels containing 0.125% chitosan may facilitate the formation of genipin/genipin cross-links between chitosan chains, further preventing formation of long regions of alginate/Ca^{2+} cross-linking. Conversely, when chitosan concentration is increased to 0.25% and genipin concentration is decreased, the Ca^{2+} concentration needed to prevent a significant change in the elastic modulus is reduced compared to hydrogels fabricated with the same alginate concentration. Increasing chitosan concentration and decreasing genipin concentration provides a higher concentration of free amine groups on the chitosan backbone and would likely lead to increased alginate/chitosan polyelectrolyte complex formation, compared to hydrogels fabricated with smaller chitosan or higher genipin concentrations. Increased polyelectrolyte complex formation would likely utilize carboxyl motifs from alginate guluronic acid residues to increase cross-linking density between alginate and chitosan chains. This would likely increase the elastic modulus of the material and lower the Ca^{2+} concentration necessary to prevent a significant change in elastic modulus.

The different cross-linking motifs exhibited within our hydrogel influence the availability of charged groups on chitosan and alginate and in turn affect the charge of the hydrogel as a whole. Thus, the charge character of composite hydrogels is largely dependent on hydrogel composition and internal cross-linking structure. Figures 6A-6C provide a schematic diagram for the proposed cross-linking mechanisms within each type of hydrogel blend and demonstrate how internal cross-linking may affect astrocyte attachment and hydrogel electrical charge. Our study demonstrated that when chitosan and genipin concentrations were kept constant, a decrease in alginate concentration caused a significant increase in free amine group concentration. This indicates that alginate chains are likely forming polyelectrolyte complexes with chitosan amine groups and decreasing positive hydrogel charge. Interestingly, for hydrogels with constant chitosan concentration, a decrease in alginate concentration supplemented with an increase in genipin concentration demonstrates a smaller increase in free amine group concentration compared to when genipin concentration was unchanged. This is not unexpected, as the resultant decrease in alginate/chitosan polyelectrolyte complex formation frees up a number of amine groups that can be utilized for chitosan/genipin cross-link formation. Similar behavior is observed when chitosan concentration is varied. When alginate concentration is kept constant, chitosan concentration is doubled and genipin concentration is decreased from 0.1% to 0.01%, a 3.4-fold increase in free amine group concentration is observed for composite hydrogels containing 0.5% alginate. Similarly, when

the genipin concentration was decreased from 0.1% to 0.05%, a 2.7-fold increase was observed for composite hydrogels containing 0.25% alginate. This indicates the concentration of genipin within alginate/chitosan/genipin hydrogels significantly impacts chitosan cross-linking and the bulk charge characteristics of hydrogels.

Furthermore, the dominant method of cross-linking within each hydrogel blend significantly affects hydrogel degradation rate. For alginate hydrogels, a relatively linear decrease in percentage of gel remaining is observed throughout the entirety of degradation. Surface degradation would likely dominate, as the dissociation of alginate/Ca^{2+} cross-links on the hydrogel surface would promote dissolution of alginate chains before Ca^{2+} ions can diffuse out of the hydrogel bulk. The inclusion of chitosan/genipin would promote the formation of alginate/chitosan polyelectrolyte complexes and chitosan/genipin cross-links, helping to keep the hydrogel intact for a longer period of time as Ca^{2+} ions diffuse out of the hydrogel bulk. Eventually, enough Ca^{2+} has diffused out of the gel that the hydrogel bulk is no longer stable and quickly degrades. This may be the reason that many alginate/chitosan hydrogels degrade slowly initially and then quickly degrade between days 14 and 21.

Rheological Characterization and Modeling of in Situ Hydrogel Behavior. Increased extracellular Ca^{2+} following initial trauma is linked to an increased incidence of neuronal apoptosis,[7,8] and interventions aimed at lowering extracellular Ca^{2+} or preventing cellular uptake demonstrate a decrease in secondary neuronal cytotoxicity.[9,10] One of the main efforts of this study was to develop and characterize a hydrogel that would interact with extracellular Ca^{2+} present within cerebrospinal fluid to spur in situ gelation. In order to approximate in situ gelation, hydrogels were exposed to CSF-like media at 37 °C containing either normal (1.8 mM) or elevated (6 mM) Ca^{2+} concentrations. Following incubation, rheological analysis was performed on hydrogels to determine if incubation in Ca^{2+} containing media provides a change in viscoelastic behavior and promotes interaction with Ca^{2+} ions present within the incubation media.

Alginate hydrogels fabricated in this study demonstrate sensitivity to changes in $CaCl_2$ concentration as small as 1 mM (Figure 1A, 1B). For both 0.25% and 0.5% alginate hydrogels, an increase in Ca^{2+} concentration during fabrication results in a significant increase in elastic modulus (Figure 1A, 1B). This implies that, at these Ca^{2+} concentrations, alginate/Ca^{2+} cross-linking sites are not saturated and that the majority of Ca^{2+} ions included during fabrication are being utilized for cross-linking. Furthermore, this implies that a number of guluronic acid residues remain available for Ca^{2+} cross-linking. Due to the homogenous nature of our material, it is highly likely that uncross-linked guluronic acid residues are exposed to the surrounding Ca^{2+} containing solution and are available for further cross-linking.

Previously, in situ gelation of alginate hydrogels for ophthalmic drug delivery was observed using simulated tears containing approximately 0.5 mM $CaCl_2$.[13] The extent of hydrogel gelation was dependent on the composition of alginate polymers. Significant gelation in situ was observed only with higher concentrations (>0.5%) of alginate polymer modified to exhibit a high concentration of guluronic acid residues (>65%). Furthermore, upon injection, the outer surface of the alginate solution cross-links instantaneously upon contact with the simulated tear solution. This promotes the formation of a strong cross-linking gradient within the hydrogel and makes the formation of a homogenously cross-linked hydrogel difficult. Additionally, this cross-linking method is more likely to saturate the alginate/Ca^{2+} cross-linking sites on the hydrogel surface and significantly decrease diffusion within the hydrogel. For example, hydrogels that were able to gel in situ within simulated tear solution demonstrated the lowest drug release rate. A hydrogel material that demonstrates homogenous physical and mechanical behavior would provide a significant benefit, as heterogeneous hydrogel properties could lead to unintended and variable cellular behavior in vivo. Using the novel fabrication method described within the text, we have developed an alginate based hydrogel system that exhibits consistent, homogenous, and controllable physical and mechanical properties while maintaining the ability to interact within Ca^{2+} ions present in the surrounding media.

Rheological studies demonstrate that these hydrogels are able to interact with calcium ions at a concentration as low as 1.8 mM in an in situ gelation model (Figure 2, Supplemental Figure 3). The linear viscoelastic limit (LVE) of a viscoelastic material is defined as the highest strain value that can be applied to a material before observing a change in elastic modulus. In the context of hydrogel materials, the magnitude of the LVE limit is associated with the structural stability of the material, the transition from a solid to a liquid like phase and material break down. For highly ordered structures, such as cross-linked hydrogels, a change in the magnitude of the LVE limit could indicate a change in the internal cross-linking structure of the hydrogel material. Rheological analysis demonstrated that all hydrogels tested within this study exhibit an increase in magnitude of the LVE limit after being incubated in media containing either normal (1.8 mM) or elevated (6 mM) levels of Ca^{2+} for a period of either two or five days at a temperature of 37 °C (Figure 2, Supplemental Figure 3). Control hydrogels that were incubated at 37 °C for their respective gelation time (in order to stabilize temperature dependent changes in viscoelastic behavior) exhibited a similar increase in elastic modulus but exhibited a lower LVE limit. Neurobasal incubation media used in this study contains various amino acids and vitamins used to promote cell growth, in addition to inorganic salts. Due to its charged nature, alginate has been shown to form polyelectrolyte complexes with other oppositely charged materials including poly (L-lysine).[52] While this type of polyelectrolyte formation would not likely increase cross-linking between alginate chains, it is possible that this type of bond formation would alter hydrogel mechanical behavior by increasing chain entanglements and decreasing the potential for structural cross-linking. Furthermore, hydrogels incubated with media containing either Ca^{2+} concentration exhibit an extended period of solidlike behavior above the LVE limit, demonstrating a significant resistance to solid-liquid phase change (Figure 2, Supplemental Figures 2 and 3). This provides further evidence for an increase in structural integrity and a change in the cross-linking behavior of hydrogels following incubation in Ca^{2+} containing media. Swelling of alginate hydrogels is significantly influenced by salt concentrations within the hydrogel and surrounding media.[53] Swelling was observed for all hydrogels during both degradation and in situ gelation experiments and would likely assist in the movement of Ca^{2+} ions into the hydrogel. Furthermore, rheological characterization demonstrated that the act of injection changes the mechanical behavior of hydrogels (data not shown). It is possible that shear thinning during injection induces a change hydrogel structure that allows for easier diffusion of Ca^{2+} into the hydrogel or allows for greater Ca^{2+} interaction within alginate cross-linking sites on the surface of the hydrogel. Injected hydrogels

were utilized for all experiments performed within this study. Together, these results provide evidence that alginate and composite hydrogels are capable of interacting with Ca^{2+} in our in situ gelation model to increase hydrogel stability by promoting further hydrogel cross-linking.

In order to determine how exposure to Ca^{2+} concentrations in CSF might influence the ultimate elastic modulus (UEM) of hydrogel blends, time tests were performed on hydrogels using our in situ gelation model with normal (1.8 mM) and elevated (6 mM) Ca^{2+} concentrations (Figure 3). The change in UEM following incubation is strongly influenced by the concentration of Ca^{2+} within the incubation media and the dominant type of cross-linking within each hydrogel. An increase in Ca^{2+} concentration within the incubation media would decrease the concentration gradient between the hydrogel and incubation media. Hydrogels exposed to elevated Ca^{2+} levels demonstrate no significant decrease in UEM at all time points (Figure 3). However, the rate of UEM decrease for hydrogels exposed to normal Ca^{2+} varies significantly depending on hydrogel composition and the dominant type of cross-linking within each type of hydrogel. For alginate hydrogels (A5/C0/G0/Ca0, Figure 3A), alginate/Ca^{2+} cross-linking is the only cross-linking mechanism present and because of the Ca^{2+} concentration gradient, the magnitude of UEM decreases quickly. When a low concentration of chitosan and a high concentration of genipin (A5/C125/G1/Ca24, Figure 3B) are added to alginate hydrogels, chitosan/genipin cross-linking dominates. A lesser amount of free amine groups remain on chitosan chains to interact with the alginate polymer, allowing for significant alginate/Ca^{2+} cross-linking to remain. While the Ca^{2+} concentration gradient allows significant degradation to take place, chitosan/genipin cross-linking, and to a lesser extent alginate/chitosan polyelectrolyte formation, maintains the UEM of the hydrogel for a longer period of time. When chitosan concentration is increased and genipin concentration is decreased (A5/C25/G01/Ca20, Figure 3C), alginate/chitosan polyelectrolyte complex formation dominates, providing a significant amount of structural integrity to the hydrogel in the presence of decreasing alginate/Ca^{2+} cross-linking, significantly inhibiting a decrease in UEM. It should be noted that the decreased elastic modulus exhibited by incubated hydrogels falls within the range reported for native CNS tissue.

Astrocyte Behavior and Drug Delivery Applications. Numerous hydrogel systems have been fabricated with the goal of increasing neuronal regeneration and neurite outgrowth following traumatic SCI.[2,3] However, the particular hydrogel material revealed here is designed with the intention of interacting with astrocytes in the acute spinal cord environment. A few studies have utilized hydrogel systems to decrease astrocyte activation and glial scar formation within in vivo models of SCI.[27,33] In one study, Khaing et al.[33] injected a high molecular weight hyaluronic acid hydrogel into a rat T8 hemisection SCI model and observed a significant decrease in glial fibrillary acidic protein (GFAP) positive cells and total chondroitin sulfate proteoglycans (CSPG) deposition. Similarly, Jain et al.[27] injected an in situ gelling agarose hydrogel containing brain derived neurotrophic factor into a similar animal model and observed a decrease in GFAP and CS-56 (CSPG) staining within the lesion site. Neuronal and glial cells respond differently to the properties of their substrate, including material stiffness. Differentiation of adult neural stem cells (aNSC) favored a neuronal phenotype when cultured on softer substrates (100−500 Pa), while substrates with an elastic modulus above 1 kPa promoted the formation of glial cultures.[54,55] These results suggest that our hydrogels may be supportive of glial cell function immediately after injection when their elastic modulus is relatively high and become increasingly supportive of axonal sprouting at longer incubation times as their elastic modulus decreases. Furthermore, hydrogel degradation has been demonstrated to facilitate the extension of neuronal process in some hydrogel systems.[56−58]

Promoting positive interaction between astrocytes and biomaterials within the spinal cord environment is critical for the success of any biomaterial-based SCI treatment. Astrocytes are often the first support cells to migrate into the biomaterial scaffold, and axonal regeneration is often observed following astrocyte migration into scaffolds.[34−36] Additionally, a material that is incompatible with astrocytes may promote the formation of reactive astrocytes, encourage formation of the glial scar, and ultimately inhibit axonal regeneration and discourage functional recovery. Furthermore, by promoting astrocyte attachment to the hydrogel surface, the potential for our hydrogel system to be used as a vehicle for delivery of therapeutic agents to astrocytes in the lesion site may be improved.

Astrocyte behavior in response to culture on hydrogel surfaces is highly dependent on hydrogel composition (Figures 6 and 7). By altering hydrogel composition, the amount of astrocyte attachment and the degree of astrocyte reactivity can be controlled. It is proposed that the dominant type of cross-linking within hydrogels is largely responsible for the differences observed in astrocyte interaction with the hydrogel surface (Figures 6A-6C). Astrocytes cultured on alginate hydrogels exhibited very low cellular attachment and demonstrated no significant increase in GFAP expression compared to astrocytes cultured on poly-D-lysine coated glass (Figures 6J and 7B). This is not an unexpected result, as the highly negatively charged nature of alginate inhibits astrocyte interaction with the hydrogel surface. The addition of 0.25% chitosan and 0.01% genipin to alginate hydrogels results in a similar number of astrocytes attached to the hydrogel surface, as compared to alginate only hydrogels (Figure 6J). However, a significant increase in number of cells per cluster was observed when astrocytes were seeded on hydrogels of this type. This clustering behavior was initially believed to be a result of the transition of cultured astrocytes to a reactive state and an increase in astrocyte proliferation. However, no significant increase in GFAP expression was observed in astrocytes cultured on hydrogels of this type, compared to alginate hydrogels and PDL coated glass. Astrocyte proliferation is observed in many types of CNS trauma and is highly correlated with severe astrogliosis and an increase in GFAP expression.[59] Healthy or mildly reactive astrocytes demonstrate relatively less GFAP expression and little to no proliferation.[60] Thus, it is unlikely that the clustering behavior observed on these hydrogels is caused by an increase in reactive astrocyte proliferation and is a result of cross-linking behavior within these hydrogels. The relatively low concentration of genipin (0.01%) leads to a high number of free amine groups (Figure 4) and the likely formation of alginate/chitosan polyelectrolyte complexes. The neutral charge of these polyelectrolyte complexes would likely be incompatible with astrocyte attachment, creating large sections of the hydrogel surface that are inhibitory for astrocyte attachment. This may be the reason that low attachment (Figure 6J) and high clustering of astrocytes (Figures 6K and 6L) is observed on these hydrogels blends, despite an overall higher positive charge (Figure 4).

A decrease in chitosan concentration (0.25% to 0.125%) along with an increase in genipin concentration (0.01% to 0.1%) provides a significant change in the behavior of astrocytes cultured on the hydrogel surface (Figures 6 and 7). Astrocytes

cultured on top of these hydrogels exhibit the highest amount of attachment, compared to alginate hydrogels and composite hydrogels with 0.25% chitosan and 0.01% genipin. In addition, astrocytes cultured on these hydrogels exhibit a significantly higher GFAP concentration than those cultured on alginate hydrogels or PDL-coated glass. Together, these results suggest that this hydrogel composition is promoting the transition of cultured astrocytes to a more reactive state, leading to a subsequent increase in astrocyte proliferation or that the hydrogel is more amenable to astrocyte attachment and astrocyte activation is a consequence of better astrocyte attachment. Astrocyte attachment is observed over the entirety of the hydrogel surface for hydrogels fabricated with 0.125% chitosan and 0.1% genipin, implying a more homogenous distribution of free amine groups on the hydrogel surface. The relatively high level of genipin would increase cross-linking between chitosan chains and increase the incidence of genipin/genipin cross-linking. Furthermore, the presence of large clusters of free amine groups would be limited, reducing the formation of large domains of alginate/chitosan polyelectrolyte complexes on the hydrogel surface. Together, these results demonstrate that hydrogel composition directly influences astrocyte attachment and activation in a composition dependent manner.

Composite images of astrocytes costained with Calcein-AM and Hoechst 33342 were created in order to determine if culture on alginate/chitosan/genipin hydrogels causes significant cell death. Calcein AM is a live cell stain that requires cellular metabolism to produce fluorescence, and Hoechst 33342 is capable of crossing the cellular membrane in both live and dead cells. Thus, cells that are costained were considered alive, while cells stained with only Hoechst 33342 were considered dead. Qualitative visualization showed a high correlation between Hoechst 33342 and Calcein AM staining. Furthermore, the concentrations of genipin used within the study are equal to or below that which has been previously used in other studies that have utilized genipin as a cross-linking agent in chitosan containing hydrogels.[18,19] These studies demonstrated significant cellular proliferation and no significant cytotoxic effects for a variety of cell types after addition of genipin to the hydrogels.

Additionally, our hydrogel blend was fabricated to interact with growth inhibitory Ca^{2+} levels in postinjury CSF not only to facilitate gelation in situ but also to help buffer out excess Ca^{2+} in an effort to reduce secondary neuronal damage during the acute and subacute phases of SCI. By reducing the magnitude of the initial increase in Ca^{2+} within CSF during the acute phase of SCI, the degree of excitotoxic secondary neuron damage would be limited. Furthermore, based on the degradation rate of alginate/chitosan hydrogels, the concentration of Ca^{2+} ions being released from the degrading hydrogel is unlikely to be significantly cytotoxic. Ca^{2+} ions would be slowly released from the degrading hydrogel into the surrounding CSF where cellular mitochondrial storage and astrocytic connections to the vascular system through the blood brain barrier would work to prevent the re-establishment of cytotoxic calcium levels. This also implies that this hydrogel system should be employed as soon as possible following the initial injury in order to be maximally effective.

These results provide for an interesting potential drug delivery application for our hydrogels during the acute/subacute phase of SCI. During these phases of SCI, astrocytes undergo a series of morphological changes and exhibit significantly modified protein expression in a process termed reactive astrogliosis.[59] A long term consequence of reactive astrocyte formation is the upregulation in production of neuronal growth inhibitory CSPGs and formation of a glial scar around the lesion site.[61] A number of studies have assessed the ability of different therapeutic agents to reduce the inhibitory nature of the glial scar.[62,63] Favorable astrocyte adhesion to hydrogels allows for astrocytes to remain in a position to readily interact with any therapeutic agents released. Furthermore, a material that allows for astrocyte adhesion without inducing significant reactive astrocyte formation would provide a significant advantage in preventing glial scar formation. All hydrogel blends examined in this study were degraded within the subacute time frame of SCI, demonstrating the potential for therapeutic delivery aimed at controlling reactive astrogliosis and CSPG content within the subacute phase of SCI. We hypothesize that our hydrogel may be a suitable platform for the delivery of therapeutic agents during the acute/subacute phase of SCI in order to reduce reactive astrogliosis and glial scar formation and encourage axonal extension into the lesion site.

5. CONCLUSIONS

The physical characteristics of alginate/chitosan/genipin composite hydrogels were characterized using small amplitude oscillatory shear rheology, degradation and ninhydrin assays, and scanning electron microscopy. Our results demonstrated that alginate/chitosan/genipin hydrogels with different compositions could be fabricated to exhibit elastic moduli similar to native spinal cord tissue. By altering hydrogel composition, the positive charge character and degradation rate of the hydrogels is variable.

Alginate/chitosan/genipin hydrogels incubated in Ca^{2+} containing, CSF-like media exhibited changes in mechanical behavior indicative of a change in the internal cross-linking structure of hydrogels in an in situ gelation model. The addition of chitosan and genipin to alginate hydrogels significantly increased hydrogel degradation time in a concentration dependent manner. Furthermore, addition of chitosan and genipin to alginate hydrogels resulted in a more positively charged hydrogel in a concentration dependent manner, indicating that hydrogel charge character can be tuned by adjusting the relative concentrations of chitosan and genipin. Astrocytes cultured on hydrogels containing chitosan and genipin demonstrated an increase in astrocyte attachment, relative to alginate hydrogels. However, this behavior decreased with increasing chitosan and decreasing genipin concentration. Additionally, astrocyte GFAP expression was dependent on hydrogel composition. An increased amount of GFAP was produced in astrocytes cultured on hydrogels demonstrating the highest degree of astrocyte attachment. This indicates that the positive charge character of the hydrogel may not be the most important factor in astrocyte compatibility, and the method of hydrogel cross-linking plays an important role in controlling astrocyte adhesion and reactivity. Together, these results demonstrate that alginate/chitosan/genipin hydrogels show great promise for facilitating interaction with and delivering therapeutic agents to astrocytes within the acutely injured spinal cord as well as providing a means to decrease Ca^{2+} related secondary neuronal damage.

■ ASSOCIATED CONTENT

Supporting Information

Figures S1 and S2 show the viscous modulus and phase angle complementary to the elastic modulus data provided in Figure 2 for hydrogels that underwent in situ gelation modeling with 1.8 mM Ca^{2+}. Figure S3 provides elastic modulus, viscous modulus, and phase angle from strain sweeps of hydrogels that underwent in situ gelation modeling with 6 mM Ca^{2+}. Figure S4

provides the complete degradation profiles for all hydrogel blends. This material is available free of charge via the Internet at http://pubs.acs.org.

AUTHOR INFORMATION

Corresponding Author

*E-mail: gilber2@rpi.edu.

Notes

The authors declare no competing financial interest.

ACKNOWLEDGMENTS

The authors would like to thank David Frey of the Rensselaer Polytechnic Institute Center for Integrated Electronics for his help with sputter coating and scanning electron microscopy. Funding for this research was provided by support from the National Institutes of Health, National Institute of Neurological Disorders and Stroke R21NS62392 to R.J.G.

REFERENCES

(1) Norenberg, M. D.; Smith, J.; Marcillo, A. *J. Neurotrauma* **2004**, *21*, 429−440.
(2) Gilbert, R. J.; Rivet, C. J.; Zuidema, J. M.; Popovich, P. G. *Crit. Rev. Biomed. Eng.* **2011**, *39*, 125−180.
(3) Macaya, D.; Spector, M. *Biomed. Mater.* **2012**, *7*, 012001.
(4) Young, W.; Yen, V.; Blight, A. *Brain Res.* **1982**, *253*, 105−113.
(5) Happel, R. D.; Smith, K. P.; Naren Banik, L.; James Powers, M.; Hogan, E. L.; Douglas Balentine, J. *Brain Res.* **1981**, *211*, 476−479.
(6) Choi, D. W. *Neurosci. Lett.* **1985**, *58*, 293−297.
(7) Wingrave, J. M.; Schaecher, K. E.; Sribnick, E. A.; Wilford, G. G.; Ray, S. K.; Hazen-Martin, D. J.; Hogan, E. L.; Banik, N. L. *J. Neurosci. Res.* **2003**, *73*, 95−104.
(8) Ray, S. K.; Hogan, E. L.; Banik, N. L. *Brain Res. Rev.* **2003**, *42*, 169−185.
(9) Limbrick, D. D., Jr.; Sombati, S.; DeLorenzo, R. J. *Cell Calcium* **2003**, *33*, 69−81.
(10) Stys, P. K.; Waxman, S. G.; Ransom, B. R. *J. Neurosci.* **1992**, *12*, 430−439.
(11) Gombotz, W.; Wee, S. *Adv. Drug Delivery Rev.* **1998**, *31*, 267−285.
(12) Prang, P.; Müller, R.; Eljaouhari, A.; Heckmann, K.; Kunz, W.; Weber, T.; Faber, C.; Vroemen, M.; Bogdahn, U.; Weidner, N. *Biomaterials* **2006**, *27*, 3560−3569.
(13) Cohen, S.; Lobel, E.; Trevgoda, A.; Peled, Y. *J. Controlled Release* **1997**, *44*, 201−208.
(14) Rowley, J. A.; Madlambayan, G.; Mooney, D. J. *Biomaterials* **1999**, *20*, 45−53.
(15) Zuidema, J. M.; Pap, M. M.; Jaroch, D. B.; Morrison, F. A.; Gilbert, R. J. *Acta Biomater.* **2011**, *7*, 1634−1643.
(16) Yamazaki, M.; Chiba, K.; Mohri, T.; Hatanaka, H. *Eur. J. Pharmacol.* **2004**, *488*, 35−43.
(17) Koo, H.-J.; Lim, K.-H.; Jung, H.-J.; Park, E.-H. *J. Ethnopharmacol.* **2006**, *103*, 496−500.
(18) Moura, M. J.; Faneca, H.; Lima, M. P.; Gil, M. H.; Figueiredo, M. M. *Biomacromolecules* **2011**, *12*, 3275−3284.
(19) Pandit, V.; Zuidema, J. M.; Venuto, K. N.; Macione, J.; Dai, G.; Gilbert, R. J.; Kotha, S. P. *Tissue Eng., Part A* **2013**, *19*, 2452−2463.
(20) Flanagan, L. A.; Ju, Y.-E.; Marg, B.; Osterfield, M.; Janmey, P. A. *Neuroreport* **2002**, *13*, 2411−2415.
(21) Balgude, A. P.; Yu, X.; Szymanski, A.; Bellamkonda, R. V. *Biomaterials* **2001**, *22*, 1077−1084.
(22) Willits, R. K.; Skornia, S. L. *J. Biomater. Sci. Polym. Ed.* **2004**, *15*, 1521−1531.
(23) Lu, Y.-B.; Franze, K.; Seifert, G.; Steinhäuser, C.; Kirchhoff, F.; Wolburg, H.; Guck, J.; Janmey, P.; Wei, E.-Q.; Käs, J.; Reichenbach, A. *Proc. Natl. Acad. Sci. U. S. A.* **2006**, *103*, 17759−17764.
(24) Hrapko, M.; van Dommelen, J. A. W.; Peters, G. W. M.; Wismans, J. S. H. M. *Biorheology* **2006**, *43*, 623−636.
(25) Banerjee, A.; Arha, M.; Choudhary, S.; Ashton, R. S.; Bhatia, S. R.; Schaffer, D. V.; Kane, R. S. *Biomaterials* **2009**, *30*, 4695−4699.
(26) Hejcl, A.; Lesný, P.; Prádný, M.; Sedý, J.; Zámecník, J.; Jendelová, P.; Michálek, J.; Syková, E. *J. Mater. Sci. Mater. Med.* **2009**, *20*, 1571−1577.
(27) Jain, A.; Kim, Y. T.; McKeon, R. J.; Bellamkonda, R. V. *Biomaterials* **2006**, *27*, 497−504.
(28) Li, X.; Liu, X.; Cui, L.; Brunson, C.; Zhao, W.; Bhat, N. R.; Zhang, N.; Wen, X. *FASEB J.* **2013**, *27*, 1127−1136.
(29) Pakulska, M. M.; Ballios, B. G.; Shoichet, M. S. *Biomed. Mater.* **2012**, *7*, 024101.
(30) Potter, W.; Kalil, R. E.; Kao, W. J. *Front. Biosci. J. Virtual Libr.* **2008**, *13*, 806−821.
(31) Katz, J. S.; Burdick, J. A. *Wiley Interdiscip. Rev. Nanomed. Nanobiotechnol.* **2009**, *1*, 128−139.
(32) Baptiste, D. C.; Fehlings, M. G. *J. Neurotrauma* **2006**, *23*, 318−334.
(33) Khaing, Z. Z.; Milman, B. D.; Vanscoy, J. E.; Seidlits, S. K.; Grill, R. J.; Schmidt, C. E. *J. Neural Eng.* **2011**, *8*, 046033.
(34) Johnson, P. J.; Parker, S. R.; Sakiyama-Elbert, S. E. *J. Biomed. Mater. Res. A* **2010**, *92A*, 152−163.
(35) Deng, L.-X.; Hu, J.; Liu, N.; Wang, X.; Smith, G. M.; Wen, X.; Xu, X.-M. *Exp. Neurol.* **2011**, *229*, 238−250.
(36) Hurtado, A.; Cregg, J. M.; Wang, H. B.; Wendell, D. F.; Oudega, M.; Gilbert, R. J.; McDonald, J. W. *Biomaterials* **2011**, *32*, 6068−6079.
(37) Andersen, T.; Strand, B. L.; Formo, K.; Alsberg, E.; Christensen, B. E. In *Carbohydrate Chemistry*; The Royal Society of Chemistry: 2012; Vol. *37*, pp 227−258.
(38) Yuan, Y.; Chesnutt, B. M.; Utturkar, G.; Haggard, W. O.; Yang, Y.; Ong, J. L.; Bumgardner, J. D. *Carbohydr. Polym.* **2007**, *68*, 561−567.
(39) Hyzinski-García, M. C.; Vincent, M. Y.; Haskew-Layton, R. E.; Dohare, P.; Keller, R. W., Jr.; Mongin, A. A *J. Neurochem.* **2011**, *118*, 140−152.
(40) Dadsetan, M.; Knight, A. M.; Lu, L.; Windebank, A. J.; Yaszemski, M. J. *Biomaterials* **2009**, *30*, 3874−3881.
(41) Dillon, G. P.; Yu, X.; Bellamkonda, R. V. *J. Biomed. Mater. Res.* **2000**, *51*, 510−519.
(42) Chen, H.; Ouyang, W.; Martoni, C.; Prakash, S. *Int. J. Polym. Sci.* **2009**, *2009*, 1−16.
(43) Chen, S.-C.; Wu, Y.-C.; Mi, F.-L.; Lin, Y.-H.; Yu, L.-C.; Sung, H.-W. *J. Controlled Release* **2004**, *96*, 285−300.
(44) Braccini, I.; Pérez, S. *Biomacromolecules* **2001**, *2*, 1089−1096.
(45) Li, L.; Fang, Y.; Vreeker, R.; Appelqvist, I.; Mendes, E. *Biomacromolecules* **2007**, *8*, 464−468.
(46) Tapia, C.; Escobar, Z.; Costa, E.; Sapag-Hagar, J.; Valenzuela, F.; Basualto, C.; Gai, M. N.; Yazdani-Pedram, M. *Eur. J. Pharm. Biopharm.* **2004**, *57*, 65−75.
(47) Sankalia, M. G.; Mashru, R. C.; Sankalia, J. M.; Sutariya, V. B. *Eur. J. Pharm. Biopharm.* **2007**, *65*, 215−232.
(48) Dare, E. V.; Griffith, M.; Poitras, P.; Kaupp, J. A.; Waldman, S. D.; Carlsson, D. J.; Dervin, G.; Mayoux, C.; Hincke, M. T. *Cells Tissues Organs* **2009**, *190*, 313−325.
(49) Macaya, D.; Ng, K. K.; Spector, M. *Adv. Funct. Mater.* **2011**, *21*, 4788−4797.
(50) Touyama, R.; Inoue, K.; Takeda, Y.; Yatsuzuka, M.; Ikumoto, T.; Moritome, N.; Shingu, T.; Yokoi, T.; Inouye, H. *Chem. Pharm. Bull. (Tokyo)* **1994**, *42*, 1571−1578.
(51) Mi, F.-L.; Shyu, S.-S.; Peng, C.-K. *J. Polym. Sci., Part A: Polym. Chem.* **2005**, *43*, 1985−2000.
(52) King, G. A.; Daugulis, A. J.; Faulkner, P.; Goosen, M. F. A. *Biotechnol. Prog.* **1987**, *3*, 231−240.
(53) Kuo, C. K.; Ma, P. X. *J. Biomed. Mater. Res. A* **2008**, *84A*, 899−907.
(54) Saha, K.; Keung, A. J.; Irwin, E. F.; Li, Y.; Little, L.; Schaffer, D. V.; Healy, K. E. *Biophys. J.* **2008**, *95*, 4426−4438.
(55) Leipzig, N. D.; Shoichet, M. S. *Biomaterials* **2009**, *30*, 6867−6878.
(56) Rizzi, S. C.; Ehrbar, M.; Halstenberg, S.; Raeber, G. P.; Schmoekel, H. G.; Hagenmüller, H.; Müller, R.; Weber, F. E.; Hubbell, J. A. *Biomacromolecules* **2006**, *7*, 3019−3029.

(57) Pittier, R.; Sauthier, F.; Hubbell, J. A.; Hall, H. *J. Neurobiol.* **2005**, *63*, 1−14.
(58) Mahoney, M. J.; Chen, R. R.; Tan, J.; Saltzman, W. M. *Biomaterials* **2005**, *26*, 771−778.
(59) Sofroniew, M. V. *Trends Neurosci.* **2009**, *32*, 638−647.
(60) Sofroniew, M. V.; Vinters, H. V. *Acta Neuropathol. (Berl.)* **2010**, *119*, 7−35.
(61) Silver, J.; Miller, J. H. *Nat. Rev. Neurosci.* **2004**, *5*, 146−156.
(62) Bradbury, E. J.; Moon, L. D. F.; Popat, R. J.; King, V. R.; Bennett, G. S.; Patel, P. N.; Fawcett, J. W.; McMahon, S. B. *Nature* **2002**, *416*, 636−640.
(63) Brown, J. M.; Xia, J.; Zhuang, B.; Cho, K.-S.; Rogers, C. J.; Gama, C. I.; Rawat, M.; Tully, S. E.; Uetani, N.; Mason, D. E.; Tremblay, M. L.; Peters, E. C.; Habuchi, O.; Chen, D. F.; Hsieh-Wilson, L. C. *Proc. Natl. Acad. Sci. U. S. A.* **2012**, *109*, 4768−4773.